Research Square

Preprints are preliminary reports that have not undergone peer review.
They should not be considered conclusive, used to inform clinical practice,
or referenced by the media as validated information.

Multi-Objective Optimization of UAV-Assisted Wireless Sensor Network Data Collection System

Hao Zhang
Chongqing Industry and Information Vocational College
Yang Peng
Chongqing Industry and Information Vocational College
Pan Zhang
Chongqing Industry and Information Vocational College
Yin Wu
willy-attake@hotmail.com
Chongqing Industry and Information Vocational College
JiangWei Li
Chongqing Industry and Information Vocational College

Article

Keywords: UAV, wireless sensor network, MOALO, PAM, energy consumption optimization

Posted Date: November 23rd, 2026

DOI: https://doi.org/10.21203/rs.3.rs-11622055/v1

License: This work is licensed under a Creative Commons Attribution 4.0 International License.
Read Full License

Additional Declarations: No competing interests reported.

Scientific Reports

Multi-Objective Optimization of UAV-Assisted Wireless Sensor Network Data Collection System

Hao Zhang . Yang Peng . Pan Zhang . Yin Wu . JiangWei Li

Abstract

In unmanned aerial vehicle assisted wireless sensor network (UAV-assisted WSN) data collection, the number of UAV hovering points induces a critical energy trade-off. Increasing hovering points reduces the forwarding burden of relay nodes and improves network energy balance, yet it extends flight trajectories and raises the UAV's energy consumption. This paper proposes IMOALO-PAM, an improved multi-objective ant lion optimizer hybridized with partitioning around medoids (PAM). A multi-constrained multi-objective energy model is formulated, with relay node average energy consumption, its standard deviation and UAV energy consumption as optimization objectives subject to node connectivity constraints. PAM clustering selects cluster centroids as candidate hovering points to reduce search dimensionality, and an adaptive boundary shrinking strategy is introduced to mitigate the premature convergence caused by PAM preprocessing. Simulation results over 30 independent runs verify that IMOALO-PAM outperforms baseline algorithms in hypervolume (HV), spacing and energy-related metrics. The obtained Pareto solutions offer multiple feasible hovering-point configurations to support flexible energy trade-off.

Keywords: UAV . wireless sensor network . MOALO . PAM . energy consumption optimization

Introduction

Traditional WSN systems rely on base stations to relay data to data centers[1,2]. On the one hand, deploying ground base stations in remote regions incurs substantial construction costs and poses maintenance challenges. On the other hand, terrestrial base stations are susceptible to natural disasters, which may trigger communication outages and render wireless sensor networks inoperable. Fortunately, unmanned aerial vehicles, featuring flexible deployment, have been widely adopted in WSNs[3-7]. As aerial mobile base stations equipped with computing resources, UAVs provide a solution to the above challenge and have attracted extensive research attention in recent years. When UAVs act as mobile data collectors, line-of-sight (LoS) transmission links can be readily established with sensor nodes[8,9], which effectively mitigates signal interference, especially in regions abundant with ground obstacles. Within UAV-assisted wireless sensor network systems, efficient data collection under limited energy constraints has become a prominent research topic for scholars.

In the UAV-assisted WSN data collection system, sensor nodes are randomly deployed within the ground monitoring area. Carrying a base station for receiving, processing and relaying data, the UAV receives data from sensor nodes and forwards it to the processing center. It can rapidly establish temporary aerial communication nodes in the monitored region to provide data transmission services for wireless sensor networks and guarantee reliable connectivity of communication links under disaster scenarios[10,11]. Nevertheless, such benefits are premised on rational energy management. When data from a large number of nodes needs to be aggregated to relay nodes, the energy of relay nodes is prone to premature depletion, which further creates energy holes and degrades network performance. Meanwhile, the UAV is constrained by its limited onboard energy, and its endurance directly restricts the coverage of a single data collection mission. Accordingly, it is necessary to explore energy optimization strategies

under the UAV-assisted WSN data collection architecture to balance energy consumption between the UAV side and the sensing layer and prolong the network lifetime[12,13].

Related Work

For research concerning UAV as aerial mobile sinks assisting data collection in wireless sensor networks, existing works on reducing and coordinating UAV-assisted WSN system energy consumption fall into three technical categories: joint energy and trajectory optimization, clustering-based dimension-reduced data collection, and energy-oriented multi-objective trajectory optimization.

(1) Joint Optimization of UAV Energy Consumption and Trajectory

Numerous studies have jointly optimized UAV energy consumption and flight trajectories to achieve near-globally optimal data collection efficiency. Zhan et al.[14] optimized hovering altitude and trajectory jointly to minimize total flight and transmission energy consumption in UAV-enabled WSNs. Baek et al.[15] and Bouhamed et al.[16] studied energy-efficient UAV routing and autonomous navigation and scheduling, respectively, for UAV energy optimization. Considering 3D channel quality. Li et al.[17] jointly optimized sensor power allocation and UAV trajectory for WSN data collection. Formulated as a constrained Steiner minimum tree problem, the problem was solved via alternating optimization, and the proposed co-design scheme achieves a higher average data collection rate than schemes with fixed power or preset trajectories. Lee et al.[18] studied a buffer-aided UAV mobile relay system with mixed FSO/RF dual-hop links. They optimized UAV trajectory for throughput maximization under buffer and delay constraints, considering both delay-limited and delay-tolerant transmission modes. Sona et al.[19] presented a UAV deployment optimizer coupled with a D2D capacity optimization algorithm. Dynamic position adjustment and energy-saving routing enhanced emergency coverage in disaster regions. Constraints including flight altitude, residual energy and coverage radius were considered, and an error-correction communication protocol was deployed to ensure reliable data exchange between UAVs and ground terminals. Cong et al.[20] proposed a bidirectional relaying scheme for multiple UAVs. They jointly optimized transmission scheduling, transmit power and UAV trajectories to facilitate information exchange among ground user pairs in the presence of UAV-to-user interference. Zhang et al.[21] developed a deep-reinforcement-learning-based data collection strategy. Using a double deep Q-network architecture, it jointly optimized UAV trajectories, device scheduling and IRS phase shifts to dynamically balance system energy consumption, communication overhead and information timeliness. Saxena et al.[22] designed a learning-based trajectory optimizer for UAV-assisted data collection to minimize UAV flight energy consumption. Hu et al.[23] constructed UAV flight paths to cut UAV energy consumption subject to minimal data collection time. Most existing UAV-WSN data collection studies focus on joint optimization of UAV trajectory, transmit power and scheduling to improve energy efficiency or throughput, yet they rarely simultaneously consider the trade-off between sensor node energy balance and UAV energy consumption under complex practical constraints.

(2) Clustering-Based UAV Data Collection and Trajectory Planning

In UAV-assisted WSN data collection research, clustering techniques are widely used to partition sensor nodes, reduce UAV waypoints, and lower the communication overhead of sensor nodes. These methods first cluster massive sensor nodes and select cluster heads or hovering points as UAV visiting locations, followed by inter-cluster trajectory planning, which alleviates the high dimensionality of the original optimization problem. Tran et al.[24] adopted the unsupervised K-means clustering method to determine the optimal number of subclusters and UAV hovering positions, and proposed trajectories from centroids to their second-nearest centroids to improve spectrum sharing efficiency. Ghorbel et al.[25] decomposed the non-convex energy consumption problem into three subproblems: clustering-based hovering-point localization, node-to-hovering-point assignment, and TSP path planning among hovering points, which significantly reduced energy consumption of UAVs and sensors. Liu et al.[26] targeted

UAV-enabled data collection for sensor networks and integrated K-means, multi-objective particle swarm optimization and ant colony optimization to collaboratively optimize the energy consumption of sensors and UAVs and decrease the power consumption of the entire collection system. The above works verified the effectiveness of the "clustering for dimension reduction + trajectory planning" paradigm. Nevertheless, most of them adopt mean-centered K-means clustering, whose centroids are arithmetic averages of the coordinates of intra-cluster nodes. Since these centroids are virtual spatial points that may not coincide with physically deployed sensors, they are not eligible for direct selection as relay nodes.

(3) Applications of Multi-Objective Optimization in UAV Energy Consumption and Trajectory

UAV-assisted WSN data collection has multiple conflicting optimization objectives. To characterize the inherent trade-offs among these objectives, some studies adopted Pareto-based multi-objective evolutionary algorithms. Yang et al.[27] formulated UAV-assisted sensor data collection as a multi-objective path planning problem to obtain compromise solutions across coverage, energy consumption, latency and other metrics. Xie et al.[28] proposed a multi-objective ant colony optimizer with adaptive coordinate method(MOACO-ACM) for multi-UAV cooperative data collection. Taking the maximum single-UAV energy consumption and task completion time as dual objectives, they sought compromise solutions and used the HV metric to evaluate the Pareto front. Singh et al.[29] proposed an NSGA-II-based multi-objective path planning framework for UAV-assisted WSN with three optimization metrics: UAV energy consumption, sensor-node energy consumption, and average RSSI. They showed that multi-objective joint optimization achieves better network lifetime and throughput compared with single-objective protocols. Medani et al.[30] further leveraged Q-learning for multi-UAV path planning and achieved substantial gains in energy consumption and task completion time for scenarios with up to 500 nodes. Chen et al.[31] presented an efficient UAV-assisted data collection scheme for large-scale WSNs. Multiple UAVs were deployed to gather data from ground sensors with unknown locations, maximizing the sensor network transmission rate via joint optimization of coverage and data rate. Singh et al.[32] took sensor-node energy consumption, network lifetime and transmission latency as joint objectives to achieve coordinated optimization of three core QoS metrics: energy consumption, latency and reliability. This work adopted a multi-objective strategy to identify optimal balance solutions among competing objectives. Zeng et al.[33] investigated UAV airborne base station networks. Subject to guaranteed user quality of experience (QoE), they jointly optimized UAV trajectories and communication resource allocation to maximize system energy efficiency. Liu et al.[34] investigated a wirelessly powered UAV-MEC system and implemented multi-objective co-optimization of communication rate, energy harvesting, energy consumption, and latency via an improved MODDPG algorithm. These works demonstrated that multi-objective evolutionary algorithms can yield non-dominated trade-off solutions for UAV--assisted WSN data collection systems. Nevertheless, most existing studies overlooked the energy consumption of the sensing layer.

As reviewed above, existing research primarily concentrates on the optimization of UAV energy consumption, data collection efficiency, and flight trajectory, with insufficient attention paid to the sensing layer. Furthermore, most of these studies adopt single-objective optimization and fail to capture the inherent trade-off between UAV-side and sensing-layer energy consumption. To overcome these limitations, this paper proposes a multi-objective optimization framework for UAV-assisted WSN data collection. A clustering strategy is introduced to reduce search dimensionality for the joint optimization of UAV flight energy consumption and WSN energy consumption. The main contributions of this work are outlined as follows:

1. A multi-objective optimization model is established for UAV-assisted WSN data collection. The total UAV energy consumption is defined as the first objective, the energy consumption of relay nodes as the second objective, and the standard deviation of relay-node energy consumption as the third objective. Meanwhile, the connectivity between sensor nodes and relay nodes, as well as the connectivity between relay nodes and the UAV communication module, are formulated as system constraints.

2. An optimization scheme based on IMOALO-PAM is proposed for UAV-assisted WSN data collection. The PAM clustering algorithm is utilized to determine the initial UAV hovering positions, which shrinks the search space of the MOALO algorithm and improves its search efficiency. This method can effectively obtain the Pareto front of the formulated optimization problem.
3. Simulation results demonstrate that the IMOALO-PAM algorithm can effectively balance multiple conflicting objectives for UAV-assisted WSN data collection and yield feasible solutions within the solution space. Over 30 independent runs, the proposed algorithm achieves better mean HV and mean Spacing metrics than the benchmark algorithms. Under identical experimental settings, it outperforms the benchmarks with respect to UAV flight path length, UAV energy consumption, and the standard deviation of relay-node energy consumption.

System Model and Problem Formulation

System Model

As illustrated in Fig. 1, the UAV-assisted WSN data collection system is depicted. The system consists of a UAV and multiple single-antenna sensor devices randomly deployed within the monitoring area. Given the limited onboard energy of the UAV, its total flight energy consumption must be constrained within the available energy budget. A fly-and-hover communication protocol is adopted in the system model[34]. To maintain stable links between ground sensors and the UAV, the UAV keeps silent for data transmission during flight and only establishes connections and receives aggregated data from relay nodes at hovering positions. Under this protocol, the complete data collection workflow is described as follows. First, relay nodes are selected from sensor nodes through clustering. Each relay node collects and aggregates data from sensors within its cluster. The UAV takes the point directly above each relay node as its hovering waypoint and visits these relay nodes sequentially according to the waypoint sequence to realize data collection and forwarding for the whole network.

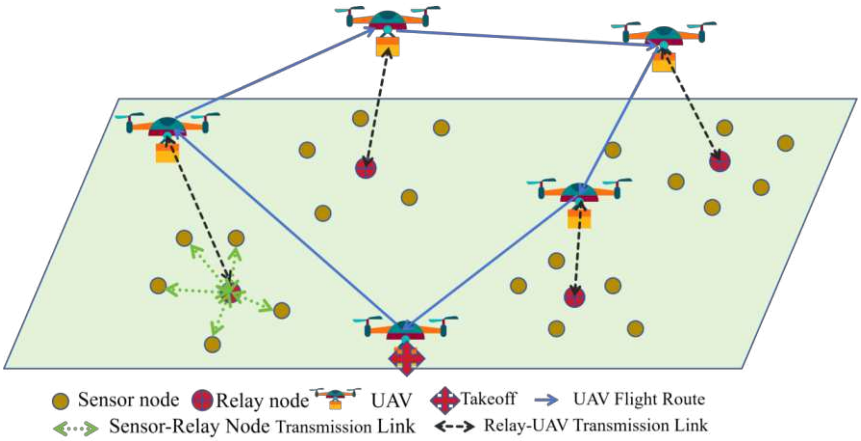


Fig. 1 System Model

In the UAV-assisted WSN data collection scenario, sensor nodes are generally deployed randomly via scattering, exhibiting scattered distribution, non-uniform density and irregular topology. Furthermore, uncoordinated transmissions from discrete nodes lack unified scheduling. When the UAV performs cruising data collection, frequent handshakes with numerous individual nodes are required, which leads to high complexity in communication scheduling and low collection efficiency. Therefore, a clustering strategy is introduced to partition randomly distributed sensor nodes into multiple subclusters. Cluster heads aggregate, fuse and forward data to the UAV base station in a unified manner. Such hierarchical transmission optimizes network topology, mitigates channel collisions and reduces node energy consumption, thereby effectively improving the stability and efficiency of system data collection.

Problem Formulation

Sensor devices: Let the ground sensor devices be denoted by $S \triangleq \{s_1, s_2, ..., s_n\}$. Each sensor node has fixed position information, and its coordinate is expressed as $[x_i, y_i, h_i]$, $s_i \in S$. These devices are randomly deployed on the ground. The deployment height of sensors can be neglected compared with the flight altitude of the UAV.

Relay devices: Let relay nodes be denoted by R, with coordinates $R \triangleq \{r_1, r_2, ..., r_m\}$, where $r_j=[x_j, y_j, h_j]$, $r_j \in R \in S$, $m \leq n$. Relay nodes are selected from sensor nodes, and they share identical physical characteristics. The connectivity between relay nodes and ordinary sensor nodes is defined as $x_{i,j} \in \{0,1\}$, $\forall i \in S, j \in R$

Each sensor node connects to at most one relay node:

$$\sum_{j \in R} x_{i,j} \leq 1 \quad \forall\, i=1, 2, ..., n \tag{1}$$

UAV: It is assumed that the UAV flies at a fixed altitude $H>0$. The UAV position set is denoted by $U=(u_0, u_1(t_1), u_2(t_2),...,u_m(t_m))$, where u_0 represents the take-off location of the UAV. The position at time instant t is written as $u(t)=[x_u(t), y_u(t), H]$. The UAV determines its next action in real time and updates its corresponding location, with the flight altitude kept constant throughout the mission.

Sensor Device Energy Consumption: Considering the complex mountainous environment, both LOS and non-line-of-sight (NLoS) transmission exist among sensor devices. This paper adopts a probabilistic LoS and NLoS path-loss model, which can accurately characterize the communication characteristics between relay nodes and sensor nodes. The LoS and NLoS path losses between a sensor node and its corresponding relay node are formulated as:

$$C_L(d)=PL(d_0)+10\alpha_L log_{10}(\frac{d_{ij}}{d_0})+\varphi^L \tag{2}$$

$$C_{NL}(d)=PL(d_0)+10\alpha_{NL} log_{10}(\frac{d_{ij}}{d_0})+\delta+\varphi^{NL} \tag{3}$$

where $PL(d_0)$ denotes the reference path loss at the reference distance, $\alpha_L$represents the LoS path loss, α_{NL}denotes the NLoS path loss, and δ is the fixed additional blocking loss for NLoS links. $\varphi^L$and $\varphi^{NL}$are the path-loss exponents for LoS and NLoS conditions, respectively, and d stands for the distance between communicating nodes. The probability of establishing a LoS link between two nodes is formulated as:

$$p_{i,j}^L=\frac{1}{1+Cexp[-D(\frac{180}{\pi}arcsin\frac{H}{d_{i,j}})-C]} \tag{4}$$

where C denotes an environmental parameter for the severity of nonlinear signal attenuation. A larger C leads to severer signal attenuation, and D quantifies the attenuation rate, with a larger D corresponding to faster signal decay. Accordingly, the probability of NLoS connectivity is given by $p_{i,j}^{NL}=1-p_{i,j}^L$. The average path loss between nodes can then be expressed as $PL_{i,j}^{AVG}=C_L p_{i,j}^L+C_{NL}p_{i,j}^{NL}$, and the path gain between nodes is formulated as:

$$g_{i,j}=\frac{P_{i,j}}{10^{PL_{i,j}^{AVG}/10}} \tag{5}$$

where $P_{i,j}$ denotes the transmit power of the sensor devices. The signal-to-noise ratio (SNR) for data transmission is formulated as:

$$SNR_{i,j}=\frac{P_{i,j}*g_{i,j}}{\overline{B_0}*N_0} \tag{6}$$

where $\overline{B_0}$ is the average bandwidth of the node, and $N_0$is the average noise power. According to the Shannon formula, the rate at which node i transmits information to node j is:

$$R_{i,j}=\overline{B_0}lg(1+SNR_{i,j}) \tag{7}$$

Assume that the length of data received by the relay node is L_j^{data}. Let T_0 and T_1 denote the time required for the relay node to establish communication channels with sensor nodes and UAV, respectively. Then the data transmission time and energy consumption of intra-cluster nodes are:

$$T_{R_j}=\frac{L_j^{data}}{R_{i,j}}+T_0 \tag{8}$$

$$E_{i,j}=P_{i,j}*T_{R_j} \tag{9}$$

When the relay node transmits data to the UAV, a line-of-sight based energy consumption transmission model is adopted. Let a_j be the length of data transmitted by the relay node. The time and transmission energy consumption between the relay node r_j and the UAV can be expressed as:

$$T_{R_j}^{UAV}=\frac{a_j*L_j^{data}}{R_{UAV,j}}+T_1 \tag{10}$$

$$E_{UAV,j}=P_{UAV,j}*T_{R_j}^{UAV} \tag{11}$$

UAV energy consumption model: Small- and medium-sized UAVs are constrained by limited onboard energy payload, short endurance and low energy efficiency. Limited by volume, weight and aerodynamic loads, battery capacity cannot be expanded indefinitely, restricting the UAV operational radius and single-mission duration[33,35]. Therefore, UAV energy optimization is of great theoretical and engineering value. UAV energy consumption includes hovering and flight energy. This work assumes fixed energy consumption for takeoff and landing, denoted as $\mathrm{P_{takeoff}}$ and $\mathrm{P_{landing}}$, respectively.

Hovering-phase energy consumption: As the basic operating state of multi-rotor UAVs, hovering has propulsion power composed of induced power and profile power.

$$P_{\mathrm{hover}}=P_{ind}+P_{pro} \tag{12}$$

The induced power is calculated based on the rotor downwash flow dynamics, with the expression:

$$P_{ind}=\frac{Mg*v_i}{\eta_{motor}} \tag{13}$$

where M denotes the total UAV mass, g the gravitational acceleration, η_{motor} is the overall efficiency of motors and electronic speed controller (ESC), and v_i is the hovering induced velocity. The hovering induced velocity v_i depends on UAV mass, air density and rotor parameters, given by:

$$v_i=\sqrt{\frac{Mg}{2\rho A_{rotor}n}} \tag{14}$$

where ρ denotes air density, A the disk area of a single rotor, and $A_{rotor}$the rotor number. The profile power describes aerodynamic drag and mechanical loss in rotor rotation, with the expression:

$$P_{pro}=\frac{\rho c_{d0}A_{blade}\chi^3R^4}{8\eta_{motor}} \tag{15}$$

where c_{d0} denotes the airfoil drag coefficient, A_{blade} the blade area, χ the rotor angular velocity, and R the rotor radius.

Flight-phase power: The UAV propulsion power during takeoff takes induced power, profile power and parasitic power into account comprehensively, with the general expression:

$$P_{\mathrm{hover}}=P_{ind}(v)+P_{pro}+P_{par}(v) \tag{16}$$

The parasitic power due to fuselage drag is:

$$P_{par}(v)=\frac{\rho C_D A_f v^3}{2\eta_m} \tag{17}$$

C_D and A_f represent the overall drag coefficient and the frontal area, respectively. In summary, the UAV flight power is given by :

$$E_{fly}=\sum_{k=1}^{K}P_{fly,k}*\triangle t_k \tag{18}$$

where $P_{fly,k}$ and $\triangle t_k$denote the k-th flight phase and corresponding duration, respectively.

Accordingly, the multi-objective optimization problem of UAV-assisted WSN data collection is formulated as Eq. 19:

$$\begin{cases} min\, f_1 = \sum_{k=1}^{K}P_{fly,k}*\triangle t_k + \int_0^{T_1}P_{\mathrm{hov}}+P_{takeoff}+P_{landing} \\ min\ f_2=(\sum_{j=1}^{m}\sum_{i=1}^{n}E_{i,j}+\sum_{j=1}^{m}E_{UAV,j})/m \\ min\, f_3 = \sqrt{\frac{1}{m}\sum_{i=1}^{m}(E_{i,j}-\overline{E})^2} \end{cases} \tag{19}$$

$$\begin{aligned} s.t\ \ & C_1:\ \textstyle\sum_{j\in R}x_{i,j}\le 1 \qquad \forall i=1,2,...,n \\ & C_2:\ E_{UAV}\ge E_{fly} \\ & C_3:\ R_c(r_j)>H \qquad \forall\, r_j\in R \\ & C_4:\ \|u_{k+1}(t_{k+1})-u_k(t_k)\|\le v_{\max}*\triangle t_k \qquad \forall \mathrm{u_k}\in U \end{aligned}$$

$$C_5: K = m+1$$

where the objective function f_1 aims to minimize the average energy consumption of relay nodes. The second objective function f_2 minimizes the standard deviation of relay node energy consumption. It is designed to improve the energy balance among relay nodes and prevent node failure caused by excessive load on a single node. The third objective function f_3 minimizes UAV energy consumption. The constraint C_1 specifies that each sensor can connect to at most one relay node to avoid extra energy loss. Another constraint C_2 ensures that the energy consumed by the UAV does not exceed its initial energy. In the constraint C_3 denotes the communication radius of relay nodes, which should be greater than the UAV flight altitude. Additional constraint C_4 limits the flight speed of the UAV. The last constraint C_5 indicates that the number of UAV hovering points is equal to the number of relay nodes.

Problem Analysis and Solution

Problem Analysis

For the first objective, lowering relay node energy consumption requires reducing their transmitted data volume, which means more relay nodes need to be deployed. For the third objective, UAV energy reduction can be achieved by shortening hovering time and reducing flight path length. Fig. 2 and Fig. 3 show two UAV-assisted data collection schemes.

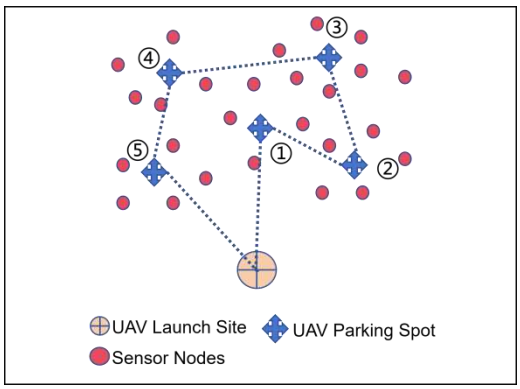


Fig. 2 Data Collection Scheme 1.

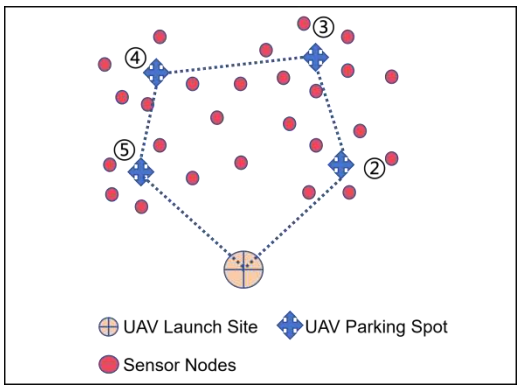


Fig. 3 Data Collection Scheme 2.

The Fig. 2 sets five hovering points for the UAV, which means the number of clusters is 5. Fig. 3 configures 4 hovering points for the UAV, one less than Fig. 2, corresponding to 4 clusters. Fig. 2 has more UAV hovering points, which leads to a longer flight path and higher UAV energy consumption compared with Fig. 3. Nevertheless, the increased hovering points reduce the average number of sensor nodes connected to each relay node, and thus the average energy consumption of relay nodes decreases significantly.

Evidently, deploying more relay nodes reduces the number of sensor nodes assigned to each relay node, which effectively lowers the energy consumption of relay nodes. Meanwhile, additional hovering points are required for the UAV, leading to an extended flight path and higher UAV energy expenditure. A trade-off therefore exists between these two objective functions: optimizing one objective will degrade the other. Hence, this problem constitutes a typical Multi-Objective Optimization Problem (MOP). Numerous scholars have investigated multi-objective optimization problems. Major research branches of multi-objective optimization include mathematical programming methods, evolutionary algorithms and intelligent optimization algorithms[36]. Among these, Pareto-dominance-based evolutionary algorithms and decomposition-based optimization frameworks have become core directions for current research and applications, as they are well suited to complex nonlinear problems.

Multi-objective optimization algorithms based on Pareto dominance search for non-dominated solutions within the solution space by simulating evolutionary or swarm iterative processes. This allows the solution set to gradually converge and spread uniformly along the true Pareto front. Their core principles are summarized below. First, the Pareto dominance relation is employed to rank solution quality and separate dominated solutions from non-dominated ones. Second, mechanisms including crowding-distance calculation and elitist preservation strategies are adopted to maintain the diversity and uniform distribution of the solution set. After iterative evolution over multiple generations, a set of widely spread and evenly distributed non-dominated optimal solutions can be acquired. Finally, decision-makers select satisfactory compromise solutions from the Pareto solution set according to practical task preferences.

Proposed Method

The multi-objective ant lion optimizer, proposed by Mirjalili, is a meta-heuristic algorithm inspired by ant lions' hunting behavior[37]. It adopts external archive, non-dominated sorting, crowding distance and elite guidance to approximate the Pareto front rapidly, featuring fast convergence, uniform solution distribution and good robustness. Nevertheless, MOALO suffers from an imbalance between global exploration and local exploitation and premature convergence. This limitation is aggravated when PAM is used for population preprocessing. To address this problem, an individual continuous shrinking boundary strategy is adopted to enhance MOALO. In the solution procedure, the PAM algorithm first clusters sensing-layer nodes and selects proper nodes in each cluster as initial relay nodes. The improved MOALO is then used for joint optimization with three objectives: total relay node energy consumption, UAV energy consumption and network energy balance. The algorithm searches the solution space through ants' random walks, updates elite ant lions based on multi-objective dominance, and saves non-dominated solutions in an external archive to maintain population diversity. After iterations, a trade-off solution is chosen from the Pareto set to generate the UAV-assisted WSN data collection strategy, which balances flight efficiency, network energy consumption and node load.

The original shrinking strategy of the ant lion trap is given by:

$$I=10^{w\frac{t}{T}}\begin{cases} w=2 & t>0.1T \\ w=3 & t>0.5T \\ w=4 & t>0.75T \\ w=5 & t>0.9T \\ w=6 & t>0.95T \end{cases} \tag{20}$$

where w denotes a constant determined by t and T with five available cases. I grows with the increasing iteration count. Accordingly, the continuous adaptive shrinking boundary is proposed:

$$I=10^{k*sin(\frac{\pi}{2}*\frac{t}{T})} \tag{21}$$

where t denotes the current iteration, T the maximum iteration, and k a coefficient set to 5 herein. For the UAV-assisted WSN data collection model, the algorithm framework is listed in the following Table 1:

Table 1. Algorithm Architecture

IMOALO-PAM Based Optimization Scheme for UAV-WSN Data Collection
Stage 1: Parameter Initialization
1: Initialize the WSN node set S, and preset the cluster number range k_1-k_2.
2: Initialize the ant population $A_{ant}=\{ant_0, ant_1, ant_2, ..., ant_N$ and ant lion population $A_{antlion}=\{antlion_0, antlion_1, antlion_2, ..., antlion_N\}$.
3: $ant_A=(m_{ant_A}, R_{ant_A})$, m_{antA} is the number of relay nodes, and R_{antA} is the set of corresponding relay node coordinate points.
4: $antlion_A=(m_{antlion_A}, R_{antlion_A})$, $m_{antlion_A}$ is the number of relay nodes, and $R_{antlion_A}$ is the set of corresponding relay node coordinate points.
5: Set the maximum iteration number T, current iteration t, decision variable dimension D, upper and

lower bounds ub, lb, and initialize the external archive ***Archive*=∅**.

Stage 2: PAM Initial Node Clustering and Pareto Archive Construction

6: While $t < T$

For every ant_i and $antlion_j$ do

7: Take m_{ant_A} from ant_i as the initial number of cluster centers for the PAM clustering algorithm and obtain the cluster centers.

8: Calculating the fitness values $F_{A_{antlion}}$ and $F_{A_{ant}}$ for ant lion and ant according to Eq.19, respectively.

9: Merge solution sets $F_{A_{ant}}$ and $F_{A_{antlion}}$, quick sorting is adopted to retain all non-dominated solutions, which are stored in the external archive to build the initial Pareto solution setArchive.

End for

Stage 3: Iterative Loop

10: Select the non-dominated solution with the optimal sparsity from the archive as the global elite ant lion $antlion_{elite}$.

11: Select the trap ant lion $antlion_{selected}$ via the roulette wheel selection.

12: Shrink the trap range according to Eq. 21 and complete the update of the ant position.

Stage 3: Individual and Pareto Front Update

13: Compare the Pareto dominance relationship between the ant and its corresponding ant lion.

If the ant solution dominates the ant lion solution

14: Replace the position of the ant lion with that of the ant.

end if

15: Update the external archive.

16: Select the individual with the optimal crowding distance from the updated archive as the new-generation elite $antlion_{elite}$.

17: t=t+1

End while

When the maximum iteration number T is satisfied, all non-dominated solutions in the external ***Archive*** form the Pareto-optimal set of IMOALO-PAM, from which decision-makers can pick trade-off solutions based on practical preferences.

Algorithm Time Complexity Analysis

The time complexity of the IMOALO-PAM algorithm is analyzed as follows. Let T denotes the maximum number of iterations of MOALO, T_P the iteration count of PAM, N the population size, n the total number of sensor nodes and M the number of optimization objectives. The time complexity of the original MOALO algorithm is $O(TNn^2)$. The IMOALO-PAM algorithm introduces a clustering algorithm to preprocess sensor nodes. The time complexity of the PAM preprocessing algorithm is $O(T_PKn^2)$. Since the optimization objects in the MOALO stage are converted to K cluster centers, the time complexity of the MOALO part becomes $O(TNK^2)$. The time complexity of the newly added optimization strategies in this paper is $O(2TN)$, which can be neglected. Therefore, the overall time complexity of the algorithm is:

$$T(\text{IMOALO-PAM}) = O(T_PKn^2) + O(TNK^2)$$

Original MOALO constructs data collection sequences using all sensor nodes. The per-iteration cost scales with n, leading to computational burden increases sharply as the WSN expands. Our IMOALO-PAM uses one-time PAM clustering to reduce n sensor nodes to K cluster centers. Despite minor one-off overhead from PAM, the MOALO iteration complexity drops from $O(TNn^2)$ to $O(TNK^2)$, significantly reducing iterative computation. For large-scale WSNs, IMOALO-PAM has lower computational cost than the original MOALO.

5. Results

Experimental Scene Setup

To validate the effectiveness of IMOALO-PAM for the established model, simulations are implemented on a MATLAB R2024a. The hardware adopts an AMD Ryzen 7 7730U with Radeon Graphics(2.00 GHz) CPU. The monitoring field is 1000×1000 m2, with 100 sensor nodes randomly deployed inside. Relay nodes are randomly chosen from sensors, and their effective communication radius is 200 m. Remaining parameters are given in the following Table 2:

Table 2 Simulation Parameters

Parameters	Values	Parameters	Values
UAV initial position	(0,0)	Population size N	100
H	100 m	***Archive***	60
UAV cruising speed v	10 m/s	**PL_d0**	40 dB
Overall drag coefficient C_D	0.3	LOS path-loss α_L	2.2
Airfoil drag coefficient c_{d0}	0.01	NLOS path-loss α_{NL}	3.8
Number of rotors n	4	φ^L	2
Rotor radius R	0.2 m	φ^{NL}	4
Rotor angular velocity χ	600 rad/s	Node transmit power P	0.02 W
Frontal area A_f	0.05 m^2	Noise power N_0	1*1e-20 W
Blade area A_{blade}	0.01 m^2	System bandwidth B	1 MHZ
Average take-off time	8 s	Packet length a_j	4000
Average landing time	8 s	Environmental parameter C	12
Range of UAV hovering points	8 - 14	Environmental parameter D	0.135

Simulation result and analysis

The resulting Pareto front is illustrated in Fig. 4, in which F1, F2, and F3 correspond to UAV energy consumption, relay node energy consumption, and the standard deviation of relay node energy consumption, respectively.

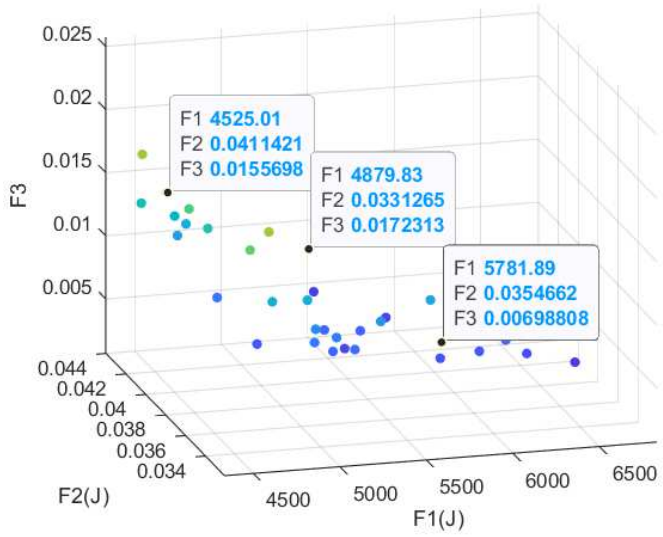


Fig. 4 Pareto Front of IMOALO-PAM Algorithm.

Three solutions $\boldsymbol{x_1}, \boldsymbol{x_2}$ and $\boldsymbol{x_3}$ are marked at the front, middle and rear of the Pareto set in Fig. 4: x_1= [4525.01, 0.0411421, 0.0155698], x_2=[4879.83, 0.0331265, 0.0172313], x_3=[5781.89, 0.0354662, 0.00698808]. x_1 achieves lower UAV energy consumption than x_2 and x_3. With fixed takeoff and landing time, x_1 contains fewer UAV hovering points. In contrast, x_2 and x_3 yield reduced relay node energy consumption. More relay nodes share the data forwarding task, so the energy consumption per relay node drops and network energy balance is improved. Accordingly, a larger number of UAV hovering points benefits relay node energy saving and network energy balance, but it increases total UAV energy consumption, which reflects the trade-off between multiple objectives.

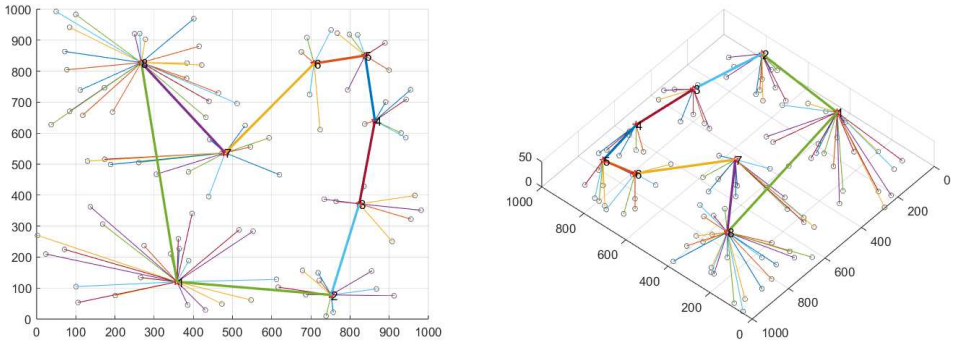


Fig. 5 UAV flight-path and clustering 2D/3D schematics with 8 hovering points.

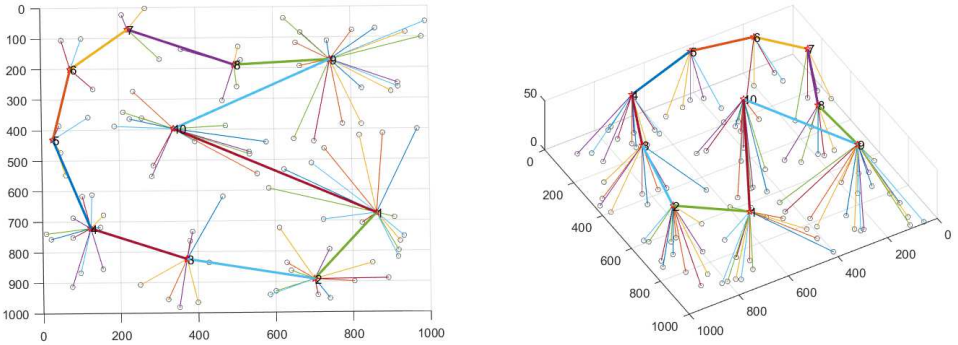


Fig. 6 UAV flight-path and clustering 2D/3D schematics with 10 hovering points.

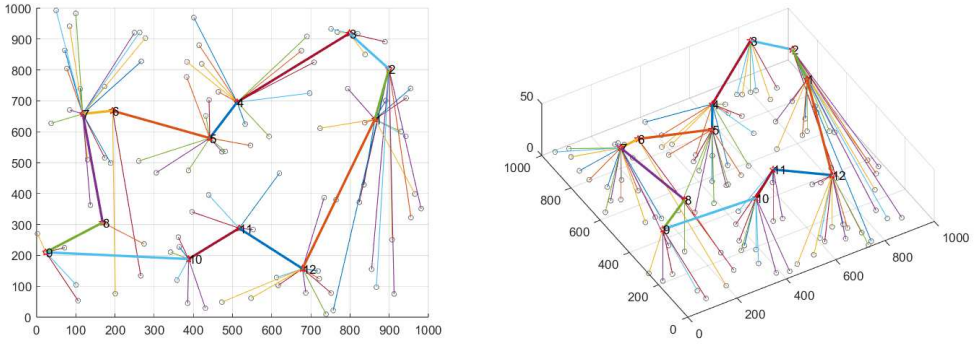


Fig. 7 UAV flight-path and clustering 2D/3D schematics with 12 hovering points.

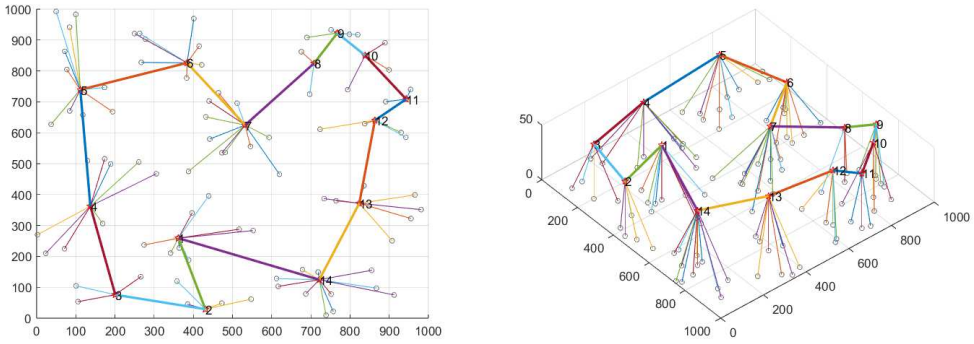
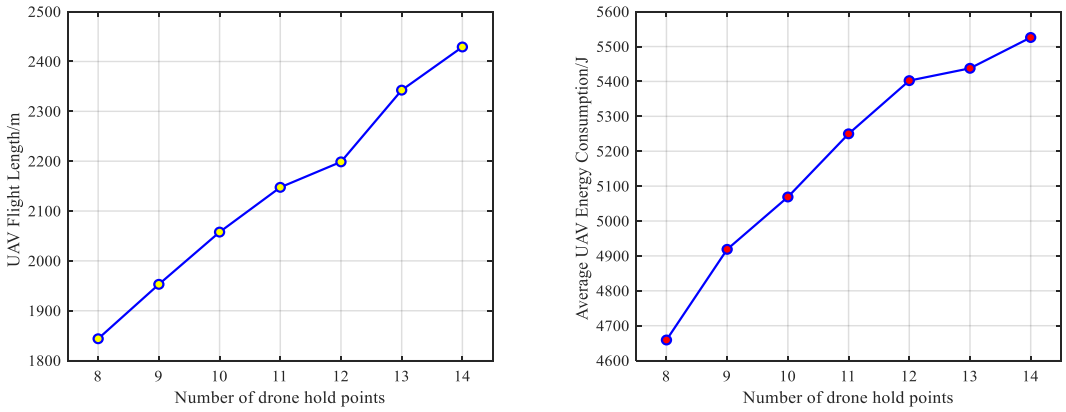


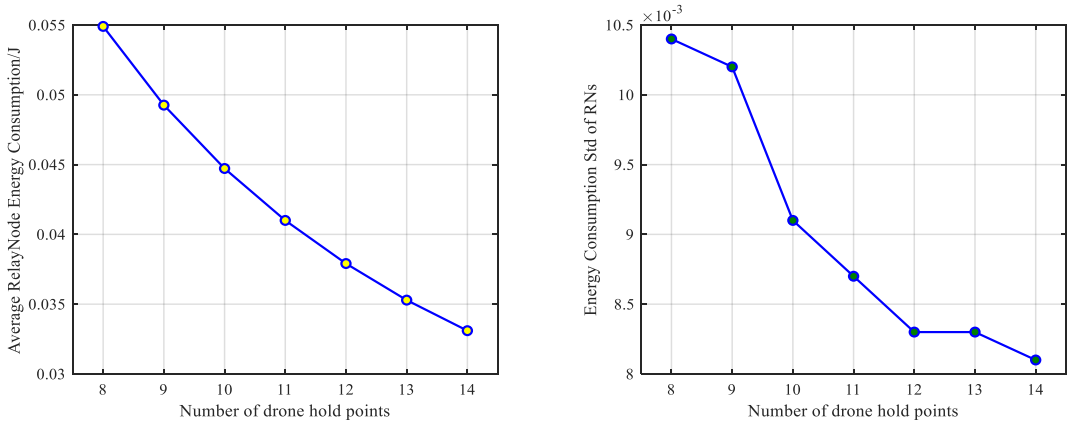
Fig. 8 UAV flight-path and clustering 2D/3D schematics with 14 hovering points.

Fig. 5, Fig. 6, Fig. 7 and Fig. 8 present the 2D and 3D schematic diagrams of UAV flight trajectories and node clustering under 8, 10, 12, 14 hovering points, respectively. In Fig. 6, each relay node forwards data for an average of 9 sensor nodes. In Fig. 8, each relay node only needs to handle data forwarding tasks for 6 sensor nodes on average. However, the UAV flight path in Fig. 6 is longer than that in Fig. 8, leading to higher UAV energy consumption.



(**a**) (**b**)

Fig. 9 Energy consumption metrics of UAV: **(a)** Variation of UAV flight path length. **(b)** Energy consumption variation of UAV.



(**a**) (**b**)

Fig. 10 Energy consumption metrics of RNs: **(a)** Energy consumption variation of RNs. **(b)** Variation of the standard deviation of energy consumption.

Fig. 9 and Fig. 10 illustrate the variation trends of relay node energy consumption, UAV energy consumption, UAV flight path length and the standard deviation of energy consumption with the number of UAV hovering points, respectively.

It can be observed from Fig. 9 and Fig. 10 that as the number of UAV hovering points increases, the energy consumption and its standard deviation of relay nodes gradually decrease, whereas the UAV flight path length and UAV energy consumption increase accordingly. This demonstrates the trade-off between different objective functions. Decision-makers may select suitable schemes for practical scenarios. When strict constraints are placed on relay node energy consumption, schemes with more hovering points can be adopted. Although these schemes yield longer UAV flight paths, they effectively reduce the energy consumption of relay nodes and improve the energy balance of the network. If the overall UAV energy consumption is the primary consideration, schemes with fewer hovering points are preferable. Such schemes shorten the UAV flight path and reduce UAV energy consumption, at the expense of higher energy consumption in the sensing layer. Naturally, a moderate compromise solution can also be chosen.

Ablation analysis

To verify the effectiveness of the proposed algorithm and its improvement strategy, ablation studies are carried out for comparisons among the proposed algorithm, MOALO, PAM, and MOALO-PAM.

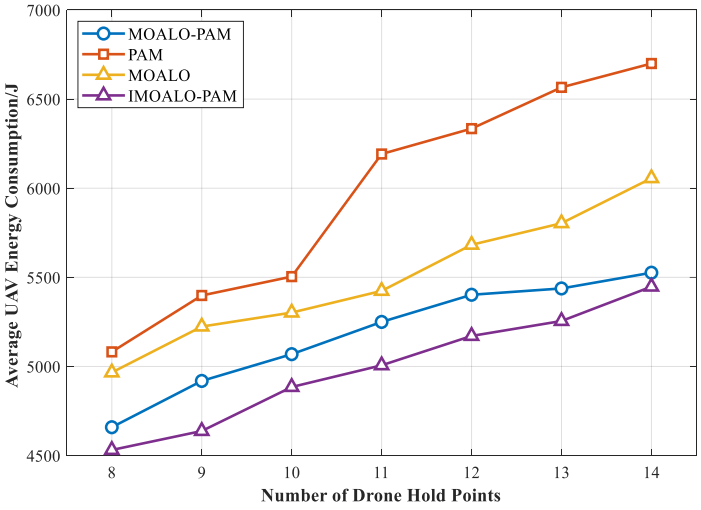


Fig. 11 UAV Flight Energy Consumption Comparison

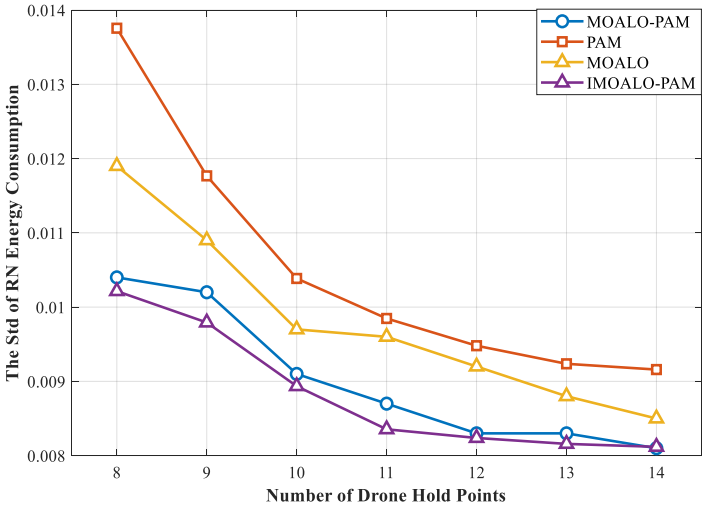


Fig. 12 Comparison of Standard Deviation of Energy Consumption for RNs

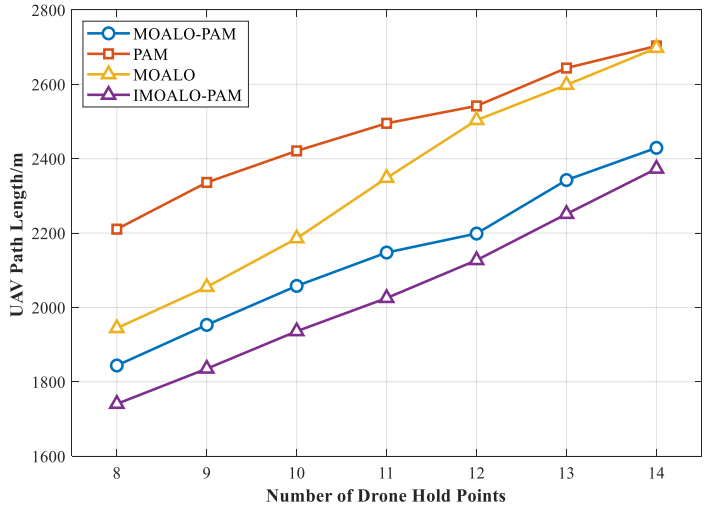


Fig. 13 Comparison of Flight Paths for UAVs

Fig. 11, Fig. 12 and Fig. 13 illustrate the comparison of corresponding metrics. Under the same number of hovering points, the IMOALO-PAM algorithm achieves noticeable improvements in terms of UAV flight path length, UAV energy consumption, and the standard deviation of relay node energy consumption, compared with MOALO-PAM, MOALO and the standalone PAM algorithms. The superior performance over MOALO-PAM demonstrates the benefit of the improvements introduced to the original MOALO, while the outperformance against MOALO and PAM verifies the effectiveness of embedding the PAM module. Collectively, these results validate the effectiveness and superiority of the proposed hybrid improvement strategy. When applied to UAV-assisted WSN data collection, the original MOALO algorithm suffers from low search efficiency and is prone to falling into local optima. By contrast, the conventional PAM algorithm optimizes cluster centers primarily based on distance metrics, leading to poor adaptability and low iterative efficiency under complex operating scenarios. By integrating the enhanced multi-objective optimization capability of the improved MOALO with the precise local path optimization and strong constraint adaptability of PAM, IMOALO-PAM effectively compensates for the inherent limitations of these individual baseline algorithms.

Benchmark Comparisons

To further verify the optimization performance of the proposed IMOALO-PAM algorithm, comparative experiments are carried out against three similar hybrid optimization algorithms: MOALO-PAM[38], MOPSO-PAM[39] and MOGWO-PAM[40]. Hypervolume (HV), Spacing, and energy-related metrics of the UAV-assisted WSN are adopted for performance evaluation. Specifically, HV quantifies the convergence of the Pareto front, while Spacing characterizes the distribution uniformity of non-dominated solutions. Table 3 lists the experimental results obtained from 30 independent algorithm runs.

Table 3. Comparison of solution sets

Algorithm	HV				Spacing			
	Mean	**Std**	**Max**	**Min**	**Mean**	**Std**	**Max**	**Min**
MOPSO-PAM	0.108	0.0478	0.15	0.01	0.0686	0.0119	0.0871	0.0528
MOALO-PAM	0.099	0.0348	0.15	0.06	0.06413	0.0082	0.0820	0.0544
MOGWO-PAM	0.127	0.0519	0.18	0.10	0.0635	0.0071	0.0750	0.0504
IMOALO-PAM	**0.141**	**0.0299**	**0.19**	**0.10**	**0.05995**	0.0077	**0.0719**	**0.0443**

IMOALO-PAM achieves the highest HV and the lowest SPACING among all competing multi-objective algorithms, demonstrating that its Pareto solution set provides better convergence and uniformity than those of the baseline algorithms. The proposed improvements effectively enhance the overall optimization performance.

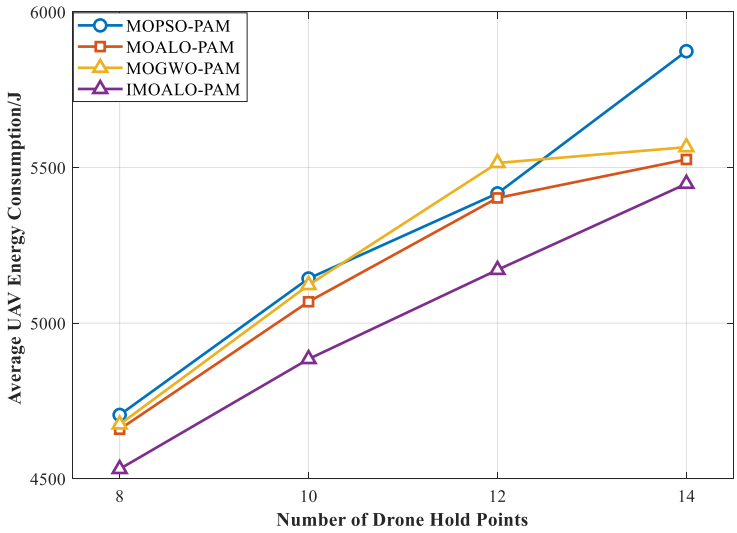


Fig. 14 Comparison of various multi-objective optimization algorithms for UAV energy.

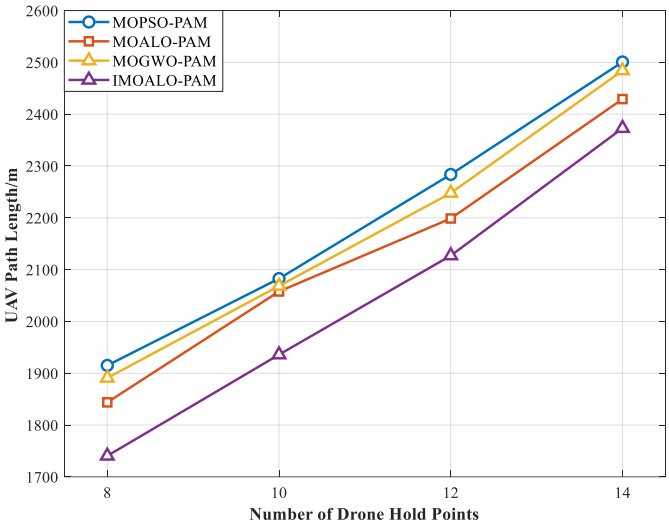


Fig. 15 Comparison of various multi-objective optimization algorithms for flight path length.

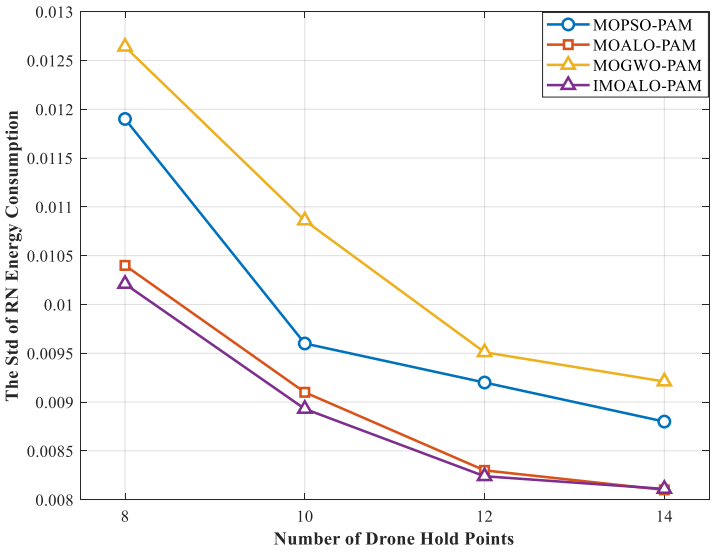


Fig. 16 Comparison of various multi-objective optimization algorithms for standard deviation of RN energy consumption.

Fig. 14, Fig. 15 and Fig. 16 plot the comparisons of UAV energy consumption, UAV flight path length, and the standard deviation of relay-node energy consumption across different algorithms. Owing to the balanced global exploration and local exploitation enabled by the continuous boundary shrinking strategy, IMOALO-PAM achieves performance improvements of different magnitudes in UAV energy consumption, flight path length, and the standard deviation of relay-node energy consumption over MOALO-PAM, MOPSO-PAM and MOGWO-PAM. It provides a superior decision space for UAV-assisted WSN data collection systems.

Discussion

This paper aims to develop a clustering-based multi-objective optimization scheme for energy consumption optimization of data collection in UAV-assisted wireless sensor networks, and validate the effectiveness of the proposed algorithm through a set of experiments.

(1) Search Dimension Reduction via PAM Algorithm

As analyzed in Chapter 4.3, the time complexity of IMOALO-PAM is $T = O(TPKn2)+O(TNK2)$. The introduction of PAM can reduce the search dimension of the MOALO algorithm. Therefore, we compare the average running time of MOALO and IMOALO-PAM over 30 independent runs under different network scales. The results are presented in the Table 4. For network sizes of 100, 150, 200 and 300 nodes, the running time of IMOALO-PAM is reduced by 35.858%, 36.652%, 34.772% and 32.219% compared with MOALO. Combined with the time complexity analysis, the embedded clustering algorithm effectively reduces the search dimension of the original algorithm and cuts down the computational time.

Table 4. Average Runtime of the Algorithm over 30 Runs under Different Numbers of Sensor Nodes

Number of Sensor Devices	Algorithm running time (s)		Percentage Reduction (%)
	MOALO	IMOALO-PAM	
100	86.919	63.978	35.858
150	89.558	65.537	36.652
200	91.423	67.835	34.772
300	94.648	71.584	32.219

(2) Ablation Experiment Analysis

To fully validate the performance improvements brought by the clustering mechanism and adaptive shrinkage strategy, this paper compares the metrics of PAM, MOALO, MOALO-PAM and IMOALO-PAM under different numbers of drone hold points.

Table 5. Average UAV energy consumption over 30 runs under PAM, MOALO, MOALO-PAM and IMOALO-PAM (J)

Drone Hold Points	PAM	MOLAO	MOALO-PAM	Percentage reduction of MOALO-PAM over MOALO (%)	IMOALO-PAM	Percentage reduction of MOALO-PAM over IMOALO-PAM (%)
8	5081.824	4966.259	4658.969	6.19	4531.356	2.74
10	5504.083	5302.210	5068.808	4.40	4884.677	3.63
12	6334.447	5682.703	5402.293	4.93	5171.147	4.28
14	6699.712	6056.204	5525.937	8.76	5447.836	1.41

Table 6. Standard deviation of relay node energy consumption 30 runs under PAM, MOALO, MOALO-PAM and IMOALO-PAM

Drone Hold Points	PAM	MOLAO	MOALO-PAM	Percentage reduction of MOALO-PAM over MOALO (%)	IMOALO-PAM	Percentage reduction of MOALO-PAM over IMOALO-PAM (%)
8	0.0118	0.0119	0.0104	6.19	0.0102	1.92
10	0.0184	0.0097	0.0091	4.40	0.0089	2.20
12	0.0142	0.0092	0.0083	4.93	0.0082	1.20
14	0.0132	0.0085	0.0081	8.76	0.0081	0.00

Table 7. UAV flight path length over 30 runs under PAM, MOALO, MOALO-PAM and IMOALO-PAM (m)

Drone Hold Points	PAM	MOLAO	MOALO-PAM	Percentage Reduction of MOALO-PAM over MOALO (%)	IMOALO-PAM	Percentage Reduction of MOALO-PAM over IMOALO-PAM (%)
8	2210.464	1944.151	1843.789	5.16	1740.478	5.60
10	2420.902	2185.605	2057.778	5.85	1935.868	5.92
12	2541.864	2503.565	2198.633	12.18	2127.025	3.26
14	2703.044	2697.661	2429.125	9.95	2372.874	2.32

The detailed experimental results are presented in Table 5, Table 6 and Table 7. The results show that MOALO-PAM achieves metric reductions of 4.40%–8.76%, 4.71%–12.61% and 5.16%–12.18% compared with the original MOALO, which demonstrates that the incorporation of PAM clustering can effectively enhance the performance of MOALO in solving the energy consumption optimization problem for UAV-assisted WSNs. Built upon the MOALO-PAM framework, IMOALO-PAM can further optimize the objective metrics, with corresponding reduction ranges of 1.41%–4.28%, 0.00%–2.20% and 2.32%–5.92%. The above ablation results verify that the proposed adaptive shrinkage strategy can yield effective performance gains for the algorithm.

(3) Experiments and Analysis on Peer Algorithms

Table 8, Table 9 and Table 10 compare the UAV energy consumption, standard deviation of relay node energy consumption and UAV flight path length of MOPSO-PAM, MOALO-PAM, MOGWO-PAM and the proposed IMOALO-PAM under different quantities of drone hold points.

Table 8. Comparison of UAV energy consumption over 30 runs for different algorithms (J)

Drone Hold Points	MOPSO-PAM	MOALO-PAM	MOGWO-PAM	IMOALO-PAM	Mean Percentage Reduction(%)
8	4705.095	4658.969	4674.588	4531.356	3.16
10	5143.367	5068.808	5122.515	4884.677	4.43
12	5417.015	5402.293	5514.691	5171.147	5.02
14	5873.807	5525.937	5565.463	5447.836	3.59

Table 9. Standard deviation comparison of relay node energy consumption over 30 runs for different algorithms

Drone Hold Points	MOPSO-PAM	MOALO-PAM	MOGWO-PAM	IMOALO-PAM	Mean Percentage Reduction(%)
8	0.0119	0.0104	0.01264	0.01021	11.75
10	0.0096	0.0091	0.01086	0.00893	8.87
12	0.0089	0.0083	0.00951	0.00824	7.16
14	0.0092	0.0081	0.00921	0.00811	7.89

Table 10. UAV flight path length comparison over 30 runs for different algorithms (m)

Drone Hold Points	MOPSO-PAM	MOALO-PAM	MOGWO-PAM	IMOALO-PAM	Mean Percentage Reduction(%)
8	1915.039	1843.789	1890.842	1740.478	7.55
10	2082.626	2057.778	2068.391	1935.868	6.46
12	2283.642	2198.633	2247.723	2127.025	5.16
14	2500.698	2429.125	2484.101	2372.874	3.97

IMOALO-PAM outperforms all peer algorithms for 8, 10, 12 and 14 drone hold points, yielding mean percentage reductions of 3.16%–5.02% in UAV energy consumption, 7.16%–11.75% in the standard deviation of relay node energy consumption, and 3.97%–7.55% in UAV flight path length. The proposed IMOALO-PAM is capable of cutting UAV energy use, shortening flight paths and stabilizing relay node energy consumption, which confirms its advantages in solving the multi-objective data collection optimization problem for UAV-assisted wireless sensor networks.

Conclusions

This study investigates the data collection optimization for UAV-assisted WSN and develops a joint optimization framework based on IMOALO-PAM to optimize the UAV flight path, UAV energy consumption, relay-node energy consumption and network energy balance simultaneously. By embedding PAM clustering, the framework selects cluster centers as candidate UAV relay nodes to reduce the search dimension. An adaptive boundary shrinkage strategy is further adopted to balance the global exploration and local exploitation of the algorithm. Simulation results validate that the proposed algorithm can yield energy-optimized schemes under diverse hovering-point configurations and supply multiple alternatives for scheduling decision-making. Benchmark comparisons with MOALO, PAM, MOALO-PAM, MOPSO-PAM and MOGWO-PAM demonstrate that IMOALO-PAM achieves superior performance in terms of UAV energy consumption, flight path length, node energy consumption and solution set distribution.

This work assumes a single UAV and stationary sensor nodes. Future research will extend the clustering framework to multi-UAV cooperative data collection, exploring joint optimization of task allocation, collision avoidance and drone hold points under energy and latency constraints. Moreover, dynamic clustering update schemes will be developed for time-varying WSNs with node failures to enable real-time re-planning of UAV hold points.

Author contributions Hao Zhang: Writing- review & editing, Methodology, Formal analysis, Conceptualization, Validation, Funding acquisition. Yang Peng: Writing-original draft, Validation, Formal analysis, Data curation, Investigation. Pan Zhang: Project administration, Supervision, Software. Jiangwei Li: Data curation, Methodology, Visualization. Yin Wu: Funding acquisition, Investigation. All authors reviewed the manuscript.

Funding This work was supported by the Science and Technology Research Program of Chongqing Municipal Education Commission (Grant Nos. KJQN202417901 & KJZD-K202517901).

Data availability The data presented in this study are available on request from corresponding author.

Competing interests The authors declare no competing interests.

References

1. Ren, J. & Li, Y. Latency-aware path planning for disconnected WSNs with mobile sinks. IEEE Wirel. Commun. Lett. 14, 2551–2555 (2025).
2. Moudoud, H., Houda, Z. A. E. & Brik, B. Advancing security and trust in WSNs: a federated multi-agent deep reinforcement learning approach. IEEE Trans. Consum. Electron. 70, 6909–6918 (2024).
3. Zeng, Y., Guo, G., Chen, S., Qiang, Y. & Liu, J. Energy-efficient data collection from UAV in WSNs based on improved PSO algorithm. IEEE Sens. J. 24, 35762–35774 (2024).
4. Bian, Y. et al. Joint trajectory control, power control, and collection schedule in UAV-assisted anti-jamming wireless data collection with imperfect CSI. IEEE Commun. Lett. 28, 2839–2843 (2024).
5. Li, J., Xie, H., Yi, H. & Lai, R. UAV-LiDAR and machine learning for estimating individual tree diameter at breast height in Chinese fir plantations approaching maturity. Remote Sens. 18, 3514 (2026).
6. Guo, Y.; Tang, Z.; Gao, C.; Xi, K.; Zuo, C. A UAV-Based Highway Slope Inspection Method Based on Multimodal Sensors and Decision-Level Fusion Strategy. Remote Sens. 2026, 18, 3407. https://doi.org/10.3390/rs18193407.
7. Moon, H. J. et al. A generalized pointing error model for FSO links with fixed-wing UAVs for 6G: analysis and trajectory optimization. IEEE Trans. Wirel. Commun. 24, 5723–5737 (2025).
8. Chen, X., Zhao, N., Chang, Z., Hämäläinen, T. & Wang, X. UAV-aided secure short-packet data collection and transmission. IEEE Trans. Commun. 71, 2475–2486 (2023).
9. Fu, Q. et al. Collection point matters in time–energy tradeoff for UAV-enabled data collection of IoT devices. IEEE Internet Things J. 11, 31492–31506 (2024).
10. Li, Y., Yao, Y., Hu, S., Wen, Q. & Zhao, F. Coverage enhancement strategy for WSNs based on multiobjective ant lion optimizer. IEEE Sens. J. 23, 13762–13773 (2023).
11. Lalhmachhuana, R. et al. Multi-objective based generation fuel cost and emission reduction using grasshopper optimization algorithm. In Proceedings of the 2023 10th International Conference on Signal Processing and Integrated Networks (SPIN), 676–680 (2023).
12. Liu, G., Cai, Z., Liang, Z. & Cheng, L. Malware suppressing strategies for smart agricultural UAV–WSN in unknown environment: a reinforcement learning framework. IEEE Internet Things J. 12, 49051–49070 (2025).
13. Song, Z., Zhang, Y., Yu, Y. & Tang, C. Cooperative positioning algorithm based on manifold gradient filtering in UAV-WSN. IEEE Sens. J. 24, 12676–12688 (2024).
14. Zhan, C., Zeng, Y. & Zhang, R. Energy-efficient data collection in UAV enabled wireless sensor network. IEEE Wirel. Commun. Lett. 7, 328–331 (2018).
15. Baek, J., Han, S. I. & Han, Y. Energy-efficient UAV routing for wireless sensor networks. IEEE Trans. Veh. Technol. 69, 1741–1750 (2019).
16. Bouhamed, O., Ghazzai, H., Besbes, H. & Massoud, Y. A UAV-assisted data collection for wireless sensor networks: autonomous navigation and scheduling. IEEE Access 8, 110446–110460 (2020).
17. Li, G., Wang, T., Wu, J. & Guan, Z. Co-design enhanced power scheme and trajectory optimization of UAV-enabled data collection from WSNs. Tsinghua Sci. Technol. 30, 2343–2365 (2025).
18. Lee, J. H., Park, K. H., Ko, Y. C. & Alouini, M. S. Throughput maximization of mixed FSO/RF UAV-aided mobile relaying with a buffer. IEEE Trans. Wirel. Commun. 20, 683–694 (2021).
19. Sona, D. R. et al. Optimized UAV-based relay algorithm for enhanced emergency wireless coverage in disaster areas. Eng. Rep. 7, e70295 (2025).
20. Cong, J. et al. Multi-UAV two-way relaying: joint scheduling, transmission power, and trajectory optimization. IEEE Trans. Veh. Technol. (2025).
21. Zhang, T. et al. Energy aware re-configurable intelligent surface assisted unmanned aerial vehicle age of information enabled data collection policies. J. Electron. Inf. Technol. 47, 427–438 (2025).
22. Saxena, K. et al. Trajectory optimization for the UAV assisted data collection in wireless sensor networks. Wirel. Netw. 28, 1785–1796 (2022).
23. Hu, Y., Liu, Y., Kaushik, A., Masouros, C. & Thompson, J. S. Timely data collection for UAV-based IoT networks: a deep reinforcement learning approach. IEEE Sens. J. 23, 12295–12308 (2023).

24. Tran, T.-N., Nguyen, T.-L., Hoang, V. T. & Voznak, M. Sensor clustering using a K-means algorithm in combination with optimized unmanned aerial vehicle trajectory in wireless sensor networks. Sensors 23, 2345 (2023).
25. Ghorbel, M. B., Rodriguez-Duarte, D., Ghazzai, H., Hossain, M. J. & Menouar, H. Joint position and travel path optimization for energy efficient wireless data gathering using unmanned aerial vehicles. IEEE Trans. Veh. Technol. 68, 2165–2175 (2019).
26. Liu, Y., Zhang, K. & Song, F. Multi-objective data collection scheme for UAV-assisted wireless sensor networks. Sci. Technol. Eng. 25, 1272–1279 (2025).
27. Yang, Q. & Yoo, S.-J. Optimal UAV path planning: sensing data acquisition over IoT sensor networks using multi-objective bio-inspired algorithms. IEEE Access 6, 13671–13684 (2018).
28. Xie, J. et al. Optimal energy and delay tradeoff in UAV-enabled wireless sensor networks. Drones 7, 368 (2023).
29. Singh, M. et al. Multi-objective NSGA-II optimization framework for UAV path planning in an UAV-assisted WSN. J. Supercomput. 79, 832–866 (2023).
30. Medani, K., Gherbi, C., Mabed, H. & Aliouat, Z. Energy-efficient Q-learning-based path planning for UAV-aided data collection in agricultural WSNs. Internet Things 33, 101698 (2025).
31. Chen, Y. et al. A deployment strategy for UAV-aided data collection in unknown environments. IEEE Sens. J. 24, 27017–27028 (2024).
32. Singh, S. P. et al. Enhancing quality of service in IoT-WSN through edge-enabled multi-objective optimization. IEEE Trans. Consum. Electron. (2025).
33. Zeng, F. et al. Resource allocation and trajectory optimization for QoE provisioning in energy-efficient UAV-enabled wireless networks. IEEE Trans. Veh. Technol. 69, 7634–7647 (2020).
34. Liu, J. et al. Multi-objective optimization for UAV-assisted wireless-powered mobile edge computing systems. J. Electron. Inf. Technol. 47, 1–14 (2025).
35. Zuo, W., Li, F. & Chu, H. H. Multi-objective optimization of micro planar combustor with tube outlet by RSM and NSGA-II for thermophotovoltaic applications. Energy 291, 130396 (2024).
36. Amooey, A. A., Mousapour, M. & Nabavi, S. R. Multiobjective particles swarm optimization and multicriteria decision making of improved cumene production process including economic, environmental, and safety criteria. Can. J. Chem. Eng. 102, 1203–1224 (2024).
37. Joshi, M. et al. Comparison of NSGA-II, MOALO and MODA for multi-objective optimization of micro-machining processes. Materials 14, 5109 (2021).
38. Schubert, E. & Rousseeuw, P. J. Fast and eager k-medoids clustering: O(k) runtime improvement of the PAM, CLARA, and CLARANS algorithms. Inf. Syst. 101, 101804 (2021).
39. Chen, S., Liu, Y., Yang, J., Ouyang, A. & Yu, J. A multi-objective particle swarm algorithm based on hierarchical clustering reference point maintenance. Sci. Rep. 15, 44751 (2025).
40. Liu, J. et al. MBB-MOGWO: modified Boltzmann-based multi-objective grey wolf optimizer. Sensors 24, 1502 (2024).

Publisher's note Springer Nature remains neutral with regard to jurisdictional claims in published maps and institutional affiliations.

Authors and Affiliations

Hao Zhang [1,3], Yang Peng [1] , Pan Zhang[1], Yin Wu[1,2], and JiangWei Li [1]

Correspondence: Yin Wu
willy-attake@hotmail.com

[1] Chongqing Industry and Information Vocational College, Chongqing 401233,China
[2] Chongqing Jiaotong University, Chongqing, 400074, China
[3] College of Electrical Engineering, Guizhou University, Guiyang 550025, China